# Pharmacokinetics and Radiation Dosimetry of $^{18}$F-Fluorocholine

Timothy R. DeGrado, PhD[1]; Robert E. Reiman, MD[2]; David T. Price, MD[3]; Shuyan Wang[1]; and R. Edward Coleman, MD[1]

*[1]Department of Radiology, Duke University Medical Center, Durham, North Carolina; [2]Division of Radiation Safety, Duke University Medical Center, Durham, North Carolina; and [3]Department of Surgery, Duke University Medical Center, Durham, North Carolina*

$^{18}$F-Fluorocholine (fluoromethyl-dimethyl-2-hydroxyethylammonium [FCH]) has been developed as an oncologic probe for PET. This study evaluates the kinetics and radiation dosimetry of $^{18}$F-FCH using murine and human biodistribution data. **Methods:** The biodistribution of $^{18}$F-FCH was obtained at time points up to 10 h after administration in control and tumor-bearing anesthetized nude mice. Human biodistribution data within the first hour after injection were obtained from attenuation-corrected whole-body PET scans of male ($n$ = 7) and female ($n$ = 5) cancer patients. Radiation dosimetry estimates were calculated using the murine and human biodistribution data assuming no redistribution of tracer after 1 h. **Results:** Rapid pharmacokinetics were observed for $^{18}$F-FCH in mice and humans. The biodistribution is nearly static after 10 min. The dose-critical organ is the kidney, which receives 0.17 ± 0.05 and 0.16 ± 0.07 mSv/MBq (0.64 ± 0.18 and 0.55 ± 0.32 rad/mCi) for females and males, respectively. The effective dose equivalent (whole body) from administration of 4.07 MBq/kg (0.110 mCi/kg) is approximately 0.01 Sv for females and males. **Conclusion:** $^{18}$F-FCH is rapidly cleared from the circulation and its biodistribution changes very slowly at >10 min after administration. The kidney is the dose-critical organ and limits administration levels of $^{18}$F-FCH to 4.07 MBq/kg (0.110 mCi/kg) in human research studies.

**Key Words:** $^{18}$F-fluorocholine; PET; oncology

**J Nucl Med 2002; 43:92–96**

Positron-labeled choline analogs are becoming increasingly useful as molecular probes for detection and localization of neoplasms in conjunction with PET (*1–7*). The avid transport of the choline analogs into malignant tissues and their rapid distribution kinetics are advantageous properties for clinical oncologic PET. However, high uptake of tracer in liver, kidney, and spleen may present limitations because of relatively high radiation doses to these tissues. This study evaluates the pharmacokinetics and biodistribution of the $^{18}$F-labeled choline analog fluoromethyl-dimethyl-2-hydroxyethylammonium (FCH) (*6,7*) in mice and humans and uses the data to calculate human radiation dosimetry estimates.

Received Mar. 19, 2001; revision accepted Sep. 21, 2001.

For correspondence or reprints contact: Timothy R. DeGrado, PhD, Department of Radiology, Duke University Medical Center, Box 3949, Durham, NC 27710.

E-mail: trd@petsparc.mc.duke.edu

## MATERIALS AND METHODS

### Synthesis of $^{18}$F-FCH

No-carrier-added $^{18}$F-FCH was synthesized through $^{18}$F-fluorobromomethane as described (*7*). The radiochemical purity was >99% by cation-exchange high-performance liquid chromatographic analysis. The final preparation consisted of $^{18}$F-FCH in sterile, isotonic saline solution.

### Biodistribution Studies in Normal and Tumor-Bearing Mice

All animal experiments were conducted under a protocol approved by the Duke University Institutional Animal Care and Use Committee. Control 4- to 6-wk-old male athymic mice (BALB/c *nu/nu*; Comprehensive Cancer Isolation Facility, Duke University Medical Center, Durham, NC) were maintained in pathogen-free conditions (*8*) without interventions. In tumor-bearing groups of mice, human cancer cells (PC-3 androgen-independent prostate carcinoma or MCF7 estrogen receptor–positive breast carcinoma; Cell Culture Facility, Duke University Medical Center, Durham, NC) were suspended in Matrigel (Collaborative Research, Bedford, MA) at a concentration of $1 \times 10^6$ cells/100 μL and were injected subcutaneously into the flank of the mice. Body weight and tumor volume were measured weekly. Tumor volume ($mm^3$) was calculated using the formula $S^2 \times L/2$, where S and L represent the large and small diameters of the tumor, respectively. After the tumor volume had surpassed 0.5 $cm^3$, the mice were anesthetized with pentobarbital (75 mg/kg) before injection of radiotracer, and they remained anesthetized throughout the study. $^{18}$F-FCH (0.74–1.48 MBq [20–40 μCi]) was injected into a tail vein. A prescribed duration of time was allowed before procurement of organs and tissues. The tissues were weighed and $^{18}$F radioactivity was measured in a γ-counter. For the bladder, the percentage of the injected dose in the urine was determined. For all other tissues, radiotracer uptake was calculated as:

$$\text{Uptake (\% dose kg/100 g)} = \frac{\text{cpm (tissue)} \times \text{Body Weight (kg)} \times 10{,}000}{\text{Tissue Weight (g)} \times \text{cpm (dose)}}, \quad \text{Eq. 1}$$

where cpm = counts per minute.

**TABLE 1**
Uptake (% Dose kg/100 g) of $^{18}$F-FCH in Tissues of Tumor-Bearing and Control Mice (male BALB/c *nu/nu*)

| | PC-3 | | | MCF7 | Control | |
|---|---|---|---|---|---|---|
| Tissue | 10 min ($n$ = 5) | 30 min ($n$ = 3) | 60 min ($n$ = 5) | 60 min ($n$ = 5) | 60 min ($n$ = 5) | 10 h ($n$ = 6) |
| Tumor | 3.6 ± 0.6 | 7.1 ± 2.1 | 7.9 ± 5.0 | 4.3 ± 1.5 | — | — |
| Blood | 2.7 ± 0.9 | 3.3 ± 0.2 | 1.5 ± 0.6 | 2.3 ± 0.5 | 1.1 ± 0.3 | 1.5 ± 0.4 |
| Heart | 15.5 ± 5.9 | 13.2 ± 2.6 | 12.7 ± 3.2 | 17.2 ± 2.5 | 18.0 ± 8.0 | 23.5 ± 5.1 |
| Brain | 0.8 ± 0.3 | 1.0 ± 0.2 | 0.8 ± 0.1 | 1.3 ± 0.4 | 1.4 ± 0.6 | 1.7 ± 0.4 |
| Lung | 18.0 ± 5.3 | 17.1 ± 1.4 | 21 ± 4.4 | 22.5 ± 2.8 | 30.2 ± 10.9 | 28.6 ± 5.8 |
| Liver | 50.7 ± 15.3 | 56.7 ± 13.2 | 58.4 ± 40.6 | 37.8 ± 13.0 | 24.5 ± 13.4 | 26.6 ± 9.8 |
| Kidney | 127.7 ± 27.6 | 116 ± 17.0 | 94.3 ± 31.0 | 99.2 ± 25.4 | 75.6 ± 25.7 | 90.6 ± 17.5 |
| Skeletal muscle | 4.4 ± 1.8 | 1.1 ± 1.0 | 4.1 ± 0.6 | 4.1 ± 0.9 | 2.2 ± 1.0 | 2.9 ± 1.0 |

### PET Studies in Patients with Prostate Cancer and Breast Cancer

The biodistribution of $^{18}$F-FCH was investigated in 7 male patients with prostate cancer and 5 female patients with breast cancer. The $^{18}$F-FCH PET studies were approved by the Duke University Medical Center Institutional Review Board and Cancer Research Committee. The subjects were informed of all risks associated with the study and written informed consent was obtained. The patients were requested to refrain from food intake for at least 4 h before scanning. No adverse events were observed in any of the patients after administration of $^{18}$F-FCH. Imaging was performed using an Advance PET scanner (General Electric Medical Systems, Milwaukee, WI) having an intrinsic spatial resolution of approximately 5 mm in all directions (*9*). Whole-body emission scans (6 or 7 bed positions × 4 min per bed position) were acquired beginning 10–20 min after administration of $^{18}$F-FCH (110–220 MBq [3–6 mCi]). Acquisition of transmission scans (6 or 7 bed positions × 3 min per bed position) followed emission imaging for correction of photon attenuation. Correction for emission activity during the transmission scan was performed using a commercially implemented algorithm. In 5 female patients, dynamic PET was performed over the heart in the first 10 min after injection to obtain time–activity curves of radioactivity in the left ventricular blood pool. Tissue concentrations of radioactivity (% dose/mL) were evaluated in various tissue regions using manual region definition on the PET images:

$$\%\ \text{Dose/mL} = \frac{C_{FCH}\ (\text{Bq/mL}) \times 100}{\text{Dose (Bq)}}, \qquad \text{Eq. 2}$$

where $C_{FCH}$ is the regional tissue concentration of radioactivity. To provide data for radiation dosimetry, the amount of radioactivity distributed to the whole organ was determined in liver, kidneys, spleen, and urinary bladder. Regions of interest around the whole organ were manually defined on the PET images by a skilled operator. For illustration purposes, the radioactivity concentration data were corrected for radioactive decay using a half-life of 109.8 min.

### Radiation Dosimetry Calculations

Human radiation dosimetry estimates based on murine biodistribution of $^{18}$F-FCH were obtained as described (*7*). Although the human biodistribution data were derived from PET studies in cancer patients, uptake of $^{18}$F-FCH by neoplasms, if present, was not considered in the dosimetry calculations. Simulation studies showed that tumor uptake, which is typically <1% of the injected dose, has a negligible effect on the calculations of the effective dose equivalent. The mean tissue activity concentrations, or fraction of dose per whole organ, were computed for females ($n$ = 5) and males ($n$ = 7). For those tissues where total organ activity was unavailable, the organ weights derived from the Cristy–Eckerman (*10*) mathematic phantoms for the adult male and the adult female were used to estimate total tissue activity. For bone and skeletal muscle, 7.2% and 40.0% of average body weight were used to estimate tissue weight (*11*).

Because the murine biodistribution data (Table 1) showed a nearly static distribution of $^{18}$F-FCH in all tissues at >10 min after administration, and initial kinetic measurements in humans using dynamic $^{18}$F-FCH PET scans corroborated these murine measurements (Fig. 1), there was no basis for considering biologic clearance in the dose calculations. All uptake was assumed to be instantaneous, and the only clearance that was considered was the physical decay of $^{18}$F (half-life = 109.8 min). The total body residence time (100% × 1.44 × half-life) was 2.64 h. The individual organ residence times were computed by multiplying the total body residence time by the fraction of administered activity that was computed for each organ. To yield a conservative estimate

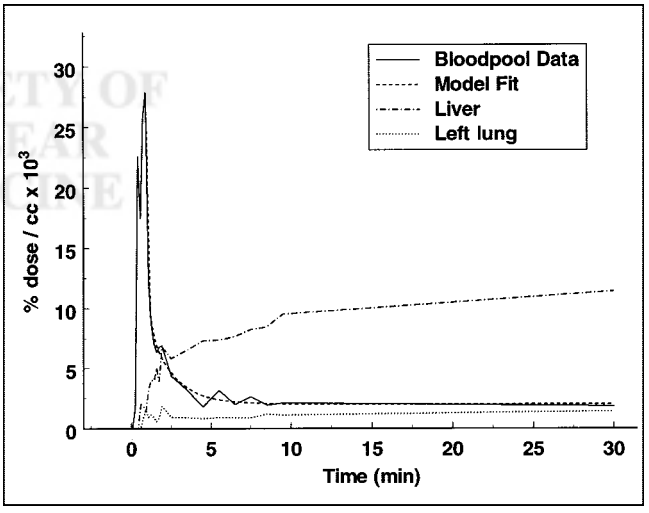


**FIGURE 1.** Pharmacokinetics of $^{18}$F-FCH in left ventricular blood pool, liver, and lung of human subject. Data are corrected for radioactive decay. Blood-pool curve is fit by multiexponential model beginning at its peak (Table 2 summarizes parameter estimates).

of radiation dose to the bladder wall and gonads, the dynamic bladder model was not used; urinary radioactivity was assumed to be present immediately after injection and not voided during the decay period of the tracer. Bone uptake was assumed to be distributed at the bone surfaces. The calculated residence times were entered into the MIRDOSE 3.1 program (*12*) to calculate dose estimates.

### Statistical Methods

Results are expressed as mean ± SD. Statistical analysis was performed using the Student *t* test and statistical significance was inferred at $P < 0.05$.

## RESULTS

### Biodistribution of $^{18}$F-FCH in Normal and Tumor-Bearing Mice

Table 1 shows the biodistribution of $^{18}$F-FCH. The kidneys and liver were the primary sites of uptake for $^{18}$F-FCH, similar to previous findings with radiolabeled choline (*1,13*). No differences were observed in biodistribution patterns found in normal tissues of control and tumor-bearing groups of mice at 1 h after administration. Also, no significant difference was found in the biodistribution of $^{18}$F-FCH between the 2 groups of mice bearing breast cancer and prostate cancer xenografts. In the prostate cancer xenograft model, the kinetics were observed to be rapid and the distribution in the tissues was essentially static after 10 min. In control mice, no significant differences were found in the biodistribution of $^{18}$F-FCH between 1 and 10 h after administration, suggesting efficient metabolic sequestration of the radiolabel in tissues consistent with previously observed lipid incorporation of the radiolabel (*7*).

### Pharmacokinetics of $^{18}$F-FCH in Human Subjects

Dynamic PET scanning that included the cardiac blood pool was performed on 5 breast cancer patients to evaluate the rapid pharmacokinetics of $^{18}$F-FCH in the blood. A region of interest was manually drawn within the left ventricular blood pool, and the dynamic PET data were evaluated from 0 to 30 min after administration (Fig. 1; Table 2). The use of image-derived blood radioactivity concentration has been validated previously against measurements using arterial blood sampling (*14*). The pharmacokinetics were fitted to a model that had 2 rapid exponential components plus a constant (Table 2). The 2 rapid phases, which were nearly complete by 3 min after administration, represented >93% of the peak radioactivity concentration. Thus, the tracer is extensively cleared in the first 5 min after administration. The concentration of $^{18}$F radioactivity in liver increased rapidly in the first 10 min and then increased slowly thereafter (Fig. 1). The concentration of $^{18}$F radioactivity in lung was relatively low at all times.

**TABLE 2**
Exponential Model Parameter Estimates for $^{18}$F-FCH Arterial Blood Clearance Kinetics

| Parameter | Value |
|---|---|
| A (% dose g/mL × $10^3$) | 18.3 ± 7.4 |
| B (1/min) | 6.13 ± 5.55 |
| C (% dose g/mL × $10^3$) | 6.29 ± 7.73 |
| D (1/min) | 0.50 ± 0.62 |
| E (% dose g/mL × $10^3$) | 1.47 ± 1.27 |
| E/(A + C + E) | 0.062 ± 0.062 |

Model: $Y$ (% dose g/mL × $10^3$) = $A \cdot e^{-B(t-p)} + C \cdot e^{-D(t-p)} + E$, where p = time of peak radioactivity concentration. $n$ = 5 patients.

**TABLE 3**
Biodistribution of $^{18}$F-FCH in Human Subjects at 10–55 Minutes After Injection

| Parameter | Female | Male |
|---|---|---|
| Subjects | | |
| *n* | 5 | 7 |
| Age (y) | 44 ± 7 | 74 ± 8 |
| Body weight (kg) | 70.8 ± 22.6 | 81.4 ± 14.0 |
| Tissue (% dose/g × $10^3$) | | |
| Myocardium | 2.52 ± 1.06 | 1.65 ± 0.51 |
| Blood | 1.62 ± 0.77 | 0.84 ± 0.28 |
| Skin | 0.36 ± 0.12 | 0.32 ± 0.08 |
| Skeletal muscle | 0.70 ± 0.27 | 0.66 ± 0.27 |
| Lung | 1.25 ± 0.44 | 1.36 ± 1.21 |
| Normal breast | 0.91 ± 0.37 | — |
| Liver | 13.52 ± 4.69 | 9.42 ± 1.90 |
| Renal cortex | 24.70 ± 13.85 | 14.95 ± 6.06 |
| Intestine | 2.22 ± 1.12 | 1.46 ± 0.85 |
| Thyroid | 2.83 ± 1.12 | 1.70 ± 0.38 |
| Salivary gland | 6.23 ± 3.26 | 3.47 ± 1.52 |
| Spleen | 7.84 ± 2.61 | 5.54 ± 2.46 |
| Normal bone | 1.17 ± 0.58 | 0.70 ± 0.23 |
| Urine | 6.34 ± 2.50 | 8.88 ± 4.36 |
| Organ (% dose/organ) | | |
| Spleen | 2.97 ± 3.46 | 1.35 ± 0.75 |
| Liver | 14.21 ± 0.84 | 13.71 ± 2.63 |
| Left kidney | 4.68 ± 1.44 | 4.48 ± 3.34 |
| Right kidney | 4.44 ± 1.25 | 3.70 ± 1.90 |
| Urinary bladder | 4.88 ± 4.79 | 1.88 ± 1.58 |

### Biodistribution of $^{18}$F-FCH in Human Subjects

Table 3 shows the uptake of $^{18}$F-FCH by various tissues in the human subjects derived from a whole-body PET scan beginning 10–20 min after administration. As noted previously (*6*), the biodistribution in humans is very similar to that in mouse with the exception of the lower lung and myocardial uptake in humans. The highest uptake was in the kidney followed by the liver and spleen. The mean activity in the bladder was 4.9% of the injected dose for females and 1.9% of the injected dose for males, although the difference was not statistically significant.

### Radiation Dosimetry Estimates

Table 4 lists the estimated radiation doses for humans in mSv/MBq (rad/mCi) administered, with the doses derived from mouse data shown for comparison. Overall, the organ doses derived from human biodistribution data are comparable to those derived from rodent tissue distribution stud-

**TABLE 4**
Radiation Dosimetry Estimates for Intravenous $^{18}$F-FCH Administration to Human Subjects on Basis of Murine and Human Biodistribution Data

| Organ or tissue | Murine data (dose per unit activity) | | Human data (dose per unit activity) | | | |
|---|---|---|---|---|---|---|
| | | | Female | | Male | |
| | mSv/MBq × $10^2$ | rad/mCi | mSv/MBq × $10^2$ | rad/mCi | mSv/MBq × $10^2$ | rad/mCi |
| Myocardium | 1.24 | 0.046 | 1.74 ± 0.31 | 0.064 ± 0.011 | 1.48 ± 0.32 | 0.048 ± 0.006 |
| Spleen | — | — | 6.37 ± 1.94 | 0.236 ± 0.072 | 5.42 ± 2.13 | 0.175 ± 0.079 |
| Small intestine | — | — | 2.57 ± 0.56 | 0.095 ± 0.021 | 2.30 ± 0.56 | 0.078 ± 0.019 |
| Uterus | — | — | 1.99 ± 0.35 | 0.074 ± 0.013 | — | — |
| Thyroid | — | — | 1.48 ± 0.34 | 0.055 ± 0.012 | 1.38 ± 0.25 | 0.049 ± 0.006 |
| Breast | — | — | 0.98 ± 0.22 | 0.036 ± 0.008 | — | — |
| Lung | 1.16 | 0.043 | 1.29 ± 0.15 | 0.048 ± 0.005 | 1.14 ± 0.28 | 0.038 ± 0.011 |
| Liver | 8.11 | 0.300 | 6.94 ± 0.41 | 0.257 ± 0.015 | 5.90 ± 1.15 | 0.191 ± 0.032 |
| Kidney | 21.90 | 0.810 | 17.35 ± 4.82 | 0.642 ± 0.178 | 15.86 ± 7.21 | 0.547 ± 0.324 |
| Bone | 1.03 | 0.038 | 2.18 ± 0.32 | 0.081 ± 0.012 | 1.91 ± 0.35 | 0.064 ± 0.008 |
| Muscle | 0.90 | 0.032 | 1.23 ± 0.14 | 0.046 ± 0.005 | 1.10 ± 0.18 | 0.037 ± 0.005 |
| Red marrow | 1.16 | 0.043 | 2.02 ± 0.18 | 0.075 ± 0.007 | 1.74 ± 0.28 | 0.057 ± 0.004 |
| Testes | 0.76 | 0.028 | — | — | 1.36 ± 0.41 | 0.039 ± 0.004 |
| Ovaries | 1.05 | 0.039 | 1.80 ± 0.15 | 0.067 ± 0.006 | — | — |
| Bladder wall | 1.32 | 0.049 | 9.66 ± 8.63 | 0.358 ± 0.319 | 6.32 ± 5.97 | 0.123 ± 0.075 |
| Effective dose equivalent | 2.97 | 0.110 | 3.69 ± 0.59 | 0.137 ± 0.022 | 3.13 ± 0.73 | 0.101 ± 0.020 |

ies. The dose-critical organ is the kidney, which receives 0.17 and 0.16 mSv/MBq (0.64 and 0.55 rad/mCi) for females and males, respectively. To comply with the 0.05-Sv single-organ dose per study limit established by the Food and Drug Administration (FDA) for research subjects, it is required that the administered activity of $^{18}$F-FCH be limited to 4.07 MBq/kg (0.110 mCi/kg) for women and 4.14 MBq/kg (0.112 mCi/kg) for men. The effective dose equivalent for humans from administration of 4.07 MBq/kg (0.110 mCi/kg) is approximately 0.01 Sv for females and males, which is below the single-study FDA limit of 0.03 Sv for research subjects.

## DISCUSSION

The rapid pharmacokinetics and long retention of $^{18}$F-FCH in tissues allow a conservative estimation of radiation doses from a model that assumes instantaneous distribution of tracer throughout the body followed by radioactive decay of $^{18}$F within the tissues. Consistent with previous $^{11}$C-choline data (*1*,*3*), blood clearance for $^{18}$F-FCH was found to be very rapid in humans with little change in the biodistribution pattern seen >10 min after administration.

Although a direct comparison of the pharmacokinetics of $^{18}$F-FCH and radiolabeled choline has not been performed in human subjects, comparison of the present data with those of Roivainen et al. (*15*) obtained with $^{11}$C-choline may suggest potential differences. Whereas $^{18}$F radioactivity concentration in arterial blood reaches a constant level >3 min after administration of $^{18}$F-FCH (*6*), the radioactivity concentration of $^{11}$C radioactivity continues to decline significantly after the early rapid clearance phase. The late clearance pattern with $^{11}$C-choline was attributed by Roivainen et al. to reflect metabolism of $^{11}$C-choline to $^{11}$C-betaine and subsequent clearance of the latter by the urinary system because most $^{11}$C in arterial plasma is in the form of $^{11}$C-betaine >5 min after administration. It is possible that $^{18}$F-FCH does not undergo similar metabolism through the oxidative pathway and therefore does not exhibit the later clearance pattern observed with $^{11}$C-choline. This notion is further supported by the finding of insignificant clearance of radiolabel in tissues of the mouse over a 10-h period after administration of $^{18}$F-FCH. Choline is known to undergo rapid oxidation in certain tissues with subsequent clearance of betaine from the tissue. For example, Haubrich et al. (*13*) observed radioactivity clearance half-lives in liver and kidney of 7–14 and 9–15 min, respectively, in guinea pigs after bolus intravenous administration of *methyl*-$^3$H-choline. Liver clearance of radioactivity was also noted for $^{11}$C-choline in PET studies of normal rabbits (*1*). The lack of tissue clearance with $^{18}$F-FCH administration may reflect specific metabolic trapping of the tracer through phosphorylation and further incorporation of the radiolabel into phospholipids as recently shown in cultured prostate cancer cells (*7*). Further analytic studies in humans are needed to confirm the suggestion that the presence of the fluorine atom of FCH renders the molecule less susceptible for oxidation (and subsequent clearance) in human tissues than natural choline.

Our data show that men and women could receive a maximum injected dose of 4.07 MBq/kg (0.110 mCi/kg) and 4.14 MBq/kg (0.112 mCi/kg), respectively, and have an acceptable dose to the kidney (0.05 Gy [5 rad]) for research studies with $^{18}$F-FCH. Thus, when the doses are expressed per gram of body weight, the limiting doses are nearly equivalent for males and females. We have chosen to take

the value of 4.07 MBq/kg (0.110 mCi/kg) as the limit for dose administration for our ongoing research studies.

The primary limitation of this study is the lack of information on the biodistribution of $^{18}$F-FCH in humans at times beyond 1 h after administration. Our assumption that there is no significant change in the tissue concentrations of tracer (correcting for decay) after a brief period is supported by the remarkably stable biodistribution of $^{18}$F-FCH in mice out to 10 h after administration. However, it is possible that species differences exist in tissue turnover of radiolabel in choline metabolite pools that we were not able to detect. A significant clearance of radiolabel from a tissue would result in a lower radiation dose in that tissue than is estimated in this study.

## CONCLUSION

Preliminary dosimetry estimates were obtained from whole-body PET studies in human subjects acquired within the first hour after tracer administration. $^{18}$F-FCH is rapidly cleared from the circulation, and its biodistribution changes very slowly $>$10 min after administration. Mouse biodistribution data showed no significant change in tissue distribution from 1 to 10 h after administration. The kidney is the dose-critical organ and limits administration levels of $^{18}$F-FCH to 4.07 MBq/kg (0.110 mCi/kg body weight) in human research studies. Dynamic PET studies on human subjects over measurement periods exceeding 1 h may provide more accurate dosimetry estimates for $^{18}$F-FCH.

## ACKNOWLEDGMENTS

The authors thank technologists Mary Hawk and DeAndre Starnes for their excellent assistance and appreciate the clinical collaborations with Drs. P. Kelly Marcom, Matthew Ellis, Michael J. Kelley, Thomas Polascik, and Cary Robertson. The authors acknowledge helpful conversations with Drs. Barbara Croft, John Hoffman, Adaline Smith, Daniel Sullivan, and James Tatum of the National Cancer Institute's Biomedical Imaging Program.

## REFERENCES

1. Hara T, Kosaka N, Shinoura N, Kondo T. PET imaging of brain tumor with [methyl-$^{11}$C]choline. *J Nucl Med*. 1997;38:842–847.
2. Shinoura N, Nishijima M, Hara T, et al. Brain tumors: detection with C-11 choline PET. *Radiology*. 1997;202:497–503.
3. Hara T, Kosaka N, Kishi H. PET imaging of prostate cancer using carbon-11-choline. *J Nucl Med*. 1998;39:990–995.
4. Kobori O, Kirihara Y, Kosaka N, Hara T. Positron emission tomography of esophageal carcinoma using $^{11}$C-choline and $^{18}$F-fluorodeoxyglucose: a novel method of preoperative lymph node staging. *Cancer*. 1999;86:1639–1648.
5. Hara T, Inagaki K, Kosaka N, Morita T. Sensitive detection of mediastinal lymph node metastasis of lung cancer with $^{11}$C-choline PET. *J Nucl Med*. 2000;41:1507–1513.
6. DeGrado TR, Coleman RE, Wang S, et al. Synthesis and evaluation of $^{18}$F-labeled choline as an oncologic tracer for positron emission tomography: initial findings in prostate cancer. *Cancer Res*. 2001;61:110–117.
7. DeGrado TR, Baldwin SW, Wang S, et al. Synthesis and evaluation of $^{18}$F-labeled choline analogs as oncologic PET tracers. *J Nucl Med*. 2001;42:1805–1814.
8. Bullard DE, Bigner DD. Heterotransplantation of human craniopharyngiomas in athymic "nude" mice. *Neurosurgery*. 1979;4:308–314.
9. DeGrado TR, Turkington TG, Williams JJ, Stearns CW, Hoffman JM, Coleman RE. Performance characteristics of a whole body PET scanner. *J Nucl Med*. 1994;35:1398–1406.
10. Cristy M, Eckerman K. *Specific Absorbed Fractions of Energy at Various Ages from Internal Photon Sources*. ORNL/TM-8381: Vol. 1–7. Oak Ridge, TN: Oak Ridge National Laboratory. 1987.
11. Task Group on Reference Man. *International Commission on Radiological Protection (ICRP) Publication 23*. Oxford, U.K.: Pergamon; 1975.
12. Stabin M. MIRDOSE: the personal computer software for use in internal dose assessment in nuclear medicine. *J Nucl Med*. 1996;37:538–546.
13. Haubrich DR, Wang PF, Wedeking PW. Distribution and metabolism of intravenously administered choline[methyl-$^{3}$H] and synthesis *in vivo* of acetylcholine in various tissues of guinea pigs. *J Pharmacol Exp Ther*. 1975;193:246–255.
14. Gambhir SS, Schwaiger M, Huang SC, et al. Simple noninvasive quantification method for measuring myocardial glucose utilization in humans employing positron emission tomography and fluorine-18 deoxyglucose. *J Nucl Med*. 1989;30:359–366.
15. Roivainen A, Forsback S, Groenroos T, et al. Blood metabolism of [*methyl*-$^{11}$C]choline: implications for in vivo imaging with positron emission tomography. *Eur J Nucl Med*. 2000;27:25–32.